University of Massachusetts Medical School

eScholarship@UMMS

Program in Molecular Medicine Publications and Presentations

Program in Molecular Medicine

2019-06-07

Smooth muscle cell-specific TMEM16A deletion does not alter Ca2+ signaling, uterine contraction, gestation length or litter size in micedagger

Mingzi Qu
University of Massachusetts Medical School

Et al.

Let us know how access to this document benefits you.

Follow this and additional works at: https://escholarship.umassmed.edu/pmm_pp

Part of the Biochemistry Commons, Cell Biology Commons, Developmental Biology Commons, Molecular Biology Commons, and the Molecular Genetics Commons

Repository Citation

Smooth muscle cell-specific TMEM16A deletion does not alter Ca^{2+} signaling, uterine contraction, gestation length or litter size in mice[ζ]

Running title. A genetic study of TMEM16A in myometrial cells

Summary sentence. The TMEM16A is absent in myometrial cells and exerts no impact on Ca^{2+} signaling, contractile responses and pregnancy in mice.

Keywords: Calcium, Ion channels, Myometrium, Uterus, Transgenic/Knockout model

Mingzi Qu[1,2], Ping Lu[2], Karl Bevell[3], Kevin Fogarty[3], Lawrence Lifshitz[3], Fangxiong Shi[1,*] and Ronghua ZhuGe[2,*]

[1]College of Animal Science and Technology, Nanjing Agricultural University, Nanjing, China. [2]Dept. of Microbiology & Physiological Systems, [3]Program in Molecular Medicine, University of Massachusetts Medical School, Worcester, Massachusetts, USA.

[*]**Correspondence:** Fangxiong Shi, Ph.D. College of Animal Science and Technology, Nanjing Agricultural University, Nanjing 210095, China. Telephone: 86 25 84399112; Email: fxshi@njau.edu.cn or Ronghua ZhuGe, Ph.D., Dept. of Microbiology & Physiological Systems, University of Massachusetts Medical School, Worcester, MA 01605, USA. Telephone: 508-856-3793, Email: Ronghua.zhuge@umassmed.edu.

Abstract

Ion channels in myometrial cells play critical roles in spontaneous and agonist-induced uterine contraction during the menstrual cycle, pregnancy maintenance and parturition; thus identifying the genes of ion channels in these cells and determining their roles are essential to understanding the biology of reproduction. Previous studies with *in vitro* functional and pharmacological approaches have produced controversial results regarding the presence and role of TMEM16A Ca^{2+}-activated Cl$^-$ channels in myometrial cells. To unambiguously determine the function of this channel in these cells,

we employed a genetic approach by using smooth muscle cell-specific TMEM16A deletion (i.e., TMEM16A^{SMKO}) mice.   We found that myometrial cells from TMEM16A^{SMKO} mice generated the same pattern and magnitude in Ca^{2+} signals upon stimulation with KCl, oxytocin and PGF2α compared to the isogenic control myometrial cells. At the uterine tissue level, TMEM16A deletion also did not cause detectable changes in either spontaneous or agonist (i.e., KCl, oxytocin and PGF2α)-induced contractions. Moreover, *in vivo* the TMEM16A^{SMKO} mice gave birth at full term with the same litter size as genetically identical control mice. Finally, TMEM16A immunostaining in both control and TMEM16A^{SMKO} mice revealed that this protein was highly expressed in the endometrial stroma, but did not co-localize with a smooth muscle specific marker MYH11. Collectively, these results unequivocally demonstrate that TMEM16A does not serve as a pacemaking channel for spontaneous uterine contraction, neither does it function as a depolarizing channel for agonist-evoked uterine contraction. Yet these two functions could underlie the normal gestation length and litter size in the TMEM16A^{SMKO} mice.

Introduction

Myometrial or uterus smooth muscle (USM) contraction and relaxation is a fundamental behavior of the uterus, essential for normal reproduction in humans. In the non-pregnant stage, USM generates peristalsis to facilitate expulsion of menses (1, 2). This peristalsis is also required for embryo implantation and pregnancy establishment. During pregnancy, USM contractile activity subsides in order to maintain pregnancy (3, 4). As pregnancy approaches full term, USM generates synchronized and coordinated contractions, leading to fetus delivery (5). Dysfunction in uterine contractility is a major cause of a variety of obstetrical and gynecological disorders such as dysmenorrhea, adenomyosis, miscarriage, preterm labor and postpartum bleeding.

USM contraction and relaxation is a highly dynamic and versatile process. Yet, in essence USM exhibits two phenotypic contractile activities, i.e., spontaneous or induced. Compelling evidence has established that ion channels are the key proteins necessary to produce both types of contractions in

the USM (3, 4, 6, 7). Therefore, it is not only physiologically but also pathologically important to identify which ion channels underlie these two types of USM contractions. Among ion channels, the presence and identity of Ca^{2+}-activated Cl^- channels (CaCCs) in the USM cells have been highly controversial and debatable. Pharmacologically, several studies demonstrated that CaCCs participate spontaneous and agonist-induced uterine contraction (8-11). Importantly, a patch clamp recording study indicated that Ca^{2+}-activated Cl^- currents are present in ~30% of rat pregnant myometrial cells(12). However, the gene identity of CaCCs in myometrial cells remains unsettled. Song et al detected CLCA4 expression and its upregulation prior to parturition in rat myometrium, suggesting that this gene may encode CaCCs in USM cells(13). But whether the CLCA family can encode *bona fide* Cl^- channels has been challenged by several studies. Mundhenk et al even found that CLCA3, a member of the CLCA family, is a secreted protein, thus it could not form an ion channel in the surface membrane (14, 15). Very recently, based on functional and pharmacological studies Bernstein et al proposed that ANO1 (TMEM16A) and ANO2 (TMEM16B) are the CaCCs in myometrial cells in mice and human(16, 17). However, Dodds et al could not detect the presence of ANO1 in mouse myometrial cells even though CaCC inhibitors can inhibit agonist-induced contraction(9). To this day, the genetic evidence for the presence of CaCCs in USM cells is lacking.

We recently used smooth muscle cell-specific TMEM16A deletion mice establishing that *Tmem16a* encodes CaCCs in smooth muscle cells from airway and internal anal sphincter (18, 19). In this study, we characterized the expression of TMEM16A and TMEM16B in mouse uteri, and studied the impact of smooth muscle specific *Tmem16a* deletion on *in vivo* reproduction behavior and *in vitro* Ca^{2+} signals and contraction responses in mice.

Materials and Methods

Mice

All experimental protocols for animal research were approved by the Institutional Animal Care and Use Committees at the University of Massachusetts Medical School (UMMS) (protocol number A1473) in accordance with the National Research Council Publication Guide for the Care and Use of Laboratory

Animals and NIH Guide for the Care and Use of Laboratory Animal. Mice were maintained under a standard 12 h light/dark cycle (lights on at 07:00 AM) with food and water ad libitum (room temperature 22 ± 2^0C). C57BL/6 mice were purchased from the Jackson Laboratory in Bar Harbor, ME, USA, and bred in the animal care facility at UMMS, Worcester, MA, USA. *Tmem16a*$^{flox/flox}$ mice with germ-line transmission were generated and confirmed by genotyping analysis and Southern blot analysis as described previously(18). To generate smooth muscle cell-specific *Tmem16a* knockout mice, *Tmem16a*$^{flox/flox}$ mice were crossed with *SMA*^{Cre} mice. *Tmem16a*$^{flox/+}$; *SMA*^{Cre} mice were used as the control and designated as TMEM16A CTR while *Tmem16a*$^{flox/flox}$; *SMA*^{Cre} mice, i.e., TMEM16A^{SMKO} mice, were used as the experimental group. TMEM16A CTR and TMEM16A^{SMKO} mutant mice were in a mixed C57BL/6 and Sv/129 background and were used at ages of 8-12 weeks.

Mouse mating and pregnancy monitoring

One-to-one pair matings were set at the end of the day. Female mice checked early the following morning with a vaginal plug were deemed a successful mating and designated as day 0 of pregnancy. Starting on day 18 of pregnancy mice were monitored twice a day for delivery.

Preparation of myometrial tissues

Female mice at estrus or at day 18 of pregnancy were euthanized by CO_2 inhalation and cervical dislocation. The estrus stage was selected because spontaneous uterine contraction in this stage is dominated by a single large spike (9) that makes frequency analysis more reliable. Uteri were quickly removed and transferred to ice-cold and oxygenated Krebs physiological buffer (KPS) which was comprised of (in mM): 118.07 NaCl, 4.69 KCl, 2.52 CaCl$_2$, 1.16 MgSO$_4$, 1.01 NaH$_2$PO$_4$, 25 NaHCO$_3$, and 11.10 glucose.

Measurement of myometrial contractility

Uteri from estrus mice were cut into circumferential rings (1.5 mm), while uteri from the antimesometrial border (i.e., the side opposite the implantation site) from d18 pregnant mice were cut into longitudinal strips (5 mm x 1.5 mm). The rings or strips were then transferred to 5-mL muscle baths containing ice cold oxygenated KPS. The rings or strips were mounted on a wire

myograph chamber (610-M, Danish Myo Technology, Aarhus, Denmark), and tension was measured by a PowerLab (ADInstruments, Colorado Springs, CO, USA) recording device. Each smooth-muscle ring or strip was equilibrated for 60 minutes with new KPS solution every 15 min, and then a 0.1 g load was applied. To test contractile responses, each ring or strip was stimulated twice with KCl (60 mM), separated by 10 min, before proceeding to other treatments. For the dose-response to KCl, each dose of KCl was added and kept for 5 min followed by three washes with KPS. For the dose-responses to oxytocin and PGF2α, either oxytocin or PGF2α was added in a cumulative manner at the concentrations as indicated in the figures. The contractile responses were calculated as area under curve (AUC), and normalized to the values (AUC/min) induced by 60 mM KCl pre-tested in the same ring or strip.

Isolation of mouse USM cells

Uteri from day 18 pregnant mice were quickly removed and placed in a pre-chilled dissociation solution consisting of (in mM): 135 NaCl, 6 KCl, 5 MgCl$_2$, 0.1 CaCl$_2$, 0.2 EDTA, 10 Hepes, and 10 glucose (pH 7.3). After gently removing the endometrium, the longitudinal myometrium were isolated and cut into strips (5 mm x 1.5 mm). The tissue strips were first incubated in a dissociation medium containing 30 unit/ml papain (Sigma-Aldrich), 1 mM DTT, and 0.5 mg/ml amino acid-free BSA (Sigma-Aldrich) at the room temperature for 30 min, and then transferred to a dissociation medium containing 3 unit/ml collagenase F (Sigma-Aldrich) and 0.5 mg/ml BSA at 35°C for another 5 min. Finally, the strips were agitated with a fire polished wide-bore glass pipette to release the cells.

Immunohistochemical analyses

Cryosections with an 8-μm thickness were fixed in pre-cooled acetone for 10 minutes and washed with PBS. The non-specific binding of primary antibodies was blocked by incubation with PBST containing 1% BSA for 1 hr. Incubation was carried out overnight at 4°C with a rabbit polyclonal antibody to TMEM16A (ab53212, 1:200; Abcam) and a mouse monoclonal antibody to MYH11 (ab683 clone 1G12, 1:200; Abcam). The specificity of these antibodies has been established by others (18, 20). After washing in PBS, cells were incubated with an Alexa Fluor 555-conjugated goat anti-Rabbit IgG (Cell

Signaling Technology, dilution 1:500) or an Alexa Fluor 488-conjugated goat anti-Mouse IgG (Cell Signaling Technology, dilution 1:500) for 1 hr. Negative controls were performed by omitting the primary antibody (Supplementary Figure 1). Immunoreactivity was evaluated using a Leica TCS SP5 confocal laser scanning microscope system (Leica Microsystems Inc., Buffalo Grove, IL, USA).

Measurement of global $[Ca^{2+}]_i$

Fluorescence images using fluo-3 as a calcium indicator were obtained using a custom-built wide-field digital imaging system. The camera was interfaced to a custom-made inverted microscope, and the cells were imaged using a 20x Nikon 1.3 NA objective for global $[Ca^{2+}]$ measurement. The 488 nm line of an Argon Ion laser provided fluorescence excitation, with a shutter to control exposure duration; emission of the Ca^{2+} indicator was monitored at wavelengths >500 nm. The images were acquired at the speed of 1 Hz for global $[Ca^{2+}]$ measurement. Subsequent image processing and analysis was performed off line using a custom-designed software package, running on a Linux/PC workstation. $[Ca^{2+}]_i$ was represented as $(F-F_0)/F_0*100$, i.e., $\Delta F/F_0*100$, where F is the fluo-3 fluorescence from entire cells in the time series and F_0 is the "resting" level derived from the same time series by computing the median value before treatments.

Reverse transcription-PCR and Quantitative Real-time PCR

The uterine endometrium and myometrium from mice were carefully isolated and quickly cleaned by removing connective tissues. Subsequently the samples were frozen and ground to homogeneity in liquid nitrogen. Total cellular RNA was isolated by using Trizol (Invitrogen, Carlsbad, CA, USA) as described in the manufacturer's instructions. Then 2μg of isolated RNA from each sample was reverse-transcribed into cDNA using SuperScript® III reverse transcriptase (Invitrogen, Carlsbad, CA, USA). The cDNA synthesis products were diluted to 200 μl, of which 1 μl was used as template for amplification of *Tmem16a* and *Tmem16b*. The housekeeping gene β-actin was used as a positive control.

Quantitative real-time PCR (qRT-PCR) was carried out to determine the mRNA levels of *Tmem16a* with iTaq™ Universal SYBR® Green Supermix (Bio-rad, Hercules, CA, USA) in accordance

with the manufacturer's protocols. The PCR cycling consisted of 40 cycles of amplification of the template cDNA with primer annealing at 60°C. Then the relative level of expression of each target gene was calculated using the $2^{-\Delta\Delta Ct}$ method. Target genes were normalized against the housekeeping gene β-actin before further analysis in Fig. 1. All the primers are listed in Supplementary Table 1.

Statistics

Unless stated otherwise, data are reported as mean ± standard error of the mean (SEM) and n represents the number of myometrial cells, uterine rings/strips, or mice. Statistical analyses of differences were carried with Student's t-test when data was from independent groups. Dose response curves had an ANOVA followed by post-hoc pair-wise t-tests at each dosing level. The significance level was set at $p<0.05$.

Results

USM cells do not express TMEM16A

TMEM16A and TMEM16B are two canonical Ca^{2+}-activated Cl^- channels (CaCCs) in a variety of cells and tissues (21-23), we therefore performed RT-PCR using endometrium and myometrium (with the serosa) from estrus and day 18 pregnant mice with specific primers for *Tmem16a* and *Tmem16b*. Figure 1A shows that positive control tissues from the eye and brain expressed both TMEM16A and TMEM16B, while myometrium and endometrium from both reproductive stages expressed TMEM16A, but not TMEM16B. To quantify TMEM16A expression, we measured TMEM16A mRNAs with quantitative PCR using endometrium and myometrium from estrus and day 18 pregnant mice. As shown in Fig. 1B, in both stages endometrium expressed more TMEM16A than myometrium, and in both tissues, TMEM16A level was higher at estrus than in day 18 pregnancy.

To determine whether USM cells express TMEM16A, we conducted dual-immunostaining of TMEM16A and MYH11 in uterine tissues from estrus and day 18 pregnant mice. MYH11 was selected because this protein is a highly specific smooth muscle cell marker(24). As expected, MYH11 staining was robustly detected in the smooth muscle layers in both estrus and day 18 pregnant mice (Figure 1C). However, essentially no TMEM16A staining can be found in the MYH11 positive smooth muscle

cells (Figure 1C). Interestingly, TMEM16A staining was detected in the stroma, but not in the luminal epithelium in both estrus and pregnant mice.

Smooth muscle cell-specific TMEM16A deletion does not change spontaneous uterine contraction in non-pregnant mice.

In our previous studies, we generated a line of mice whose TMEM16A in smooth muscle cells was specifically deleted with the LoxP-Cre technology (18). With these mice, we have successfully established that TMEM16A encodes CaCCs in smooth muscle cells from airway smooth muscle and internal anal sphincter (18, 19). Because no TMEM16B is expressed in the myometrium from both reproductive stages, we used TMEM16A[SMKO] mice to study the role, if any, of TMEM16A in USM cells. We first examined its potential effect on spontaneous contraction. In our preliminary study of CTR mice, we noticed that both isolated uterine circular rings from estrus and longitudinal strips from day 18 pregnant mice generated spontaneous contraction, but after equilibrating for 60 min, the contractions from the pregnant mice eased while it persisted for several hours in the uterine circular rings from estrus mice. Hence we focused on examining the effect of TMEM16A deletion on spontaneous contraction in the estrus stage. To quantify this effect, we calculated the contraction activity in the first 10 min post-equilibrium. As shown in Figure 2, the frequency of spontaneous contraction in the TMEM16A[SMKO] mice was 0.055 ± 0.005 Hz which was not significantly different from 0.064 ± 0.006 Hz in the CTR mice (n=20 uterine circular rings from 5 mice, P>0.05). To minimize the variation in the force due to the factors such as ring size and contamination of endometrium, we compared the force differences in the spontaneous contraction after normalizing with 60 mM KCl. In the CTR mice, the spontaneous contraction was 63.5 ± 5.1% of KCl-induced contraction, and in the TMEM16A[SMKO] mice, this value was 61.5 ± 3.0% (n=20 uterine circular rings from 5 mice, P>0.05 CTR vs TMEM16A[SMKO]).

Smooth muscle cell-specific TMEM16A deletion exerts no change in KCl-induced contraction.

Considering controversial results on the role of TMEM16A in the evoked uterine force generation, we assessed the effect of its deletion in smooth muscle cells on the contraction induced by KCl and contractile agonists (see below). In uterine circular rings at estrus from the CTR mice, KCl at

10 mM caused a substantial contraction (i.e., 36.3 ± 5.1% of 60 mM KCl-induced contraction), and as

its concentration was incrementally raised to 40 mM, KCl caused a dose-dependent contraction to

reach 95.9 ± 5.2% of the 60 mM KCl-induced contraction. Beyond 40 mM, KCl-induced contraction

was inversely related to its concentration, i.e., the higher the concentration, the less the contraction (At

120 mM, KCl caused 54.0 ± 4.6% of the 60 mM-induced contraction) (Figure 3A). The same KCl-

induced dose response curve was observed in uterine circular rings from TMEM16A[SMKO] mice (Figure

3A).

In day 18 pregnant CTR mice, KCl at 10 mM caused a marginal contraction (i.e., 4.6 ± 2.6% of

the 60 mM KCl-induced contraction) in uterine longitudinal strips. Yet, it induced markedly larger

contractions at 20 mM (71.1 ± 3.3% of the 60 mM KCl-induced contraction) and at 40 mM (131.2 ±

3.1% of the 60 mM KCl-induced contraction). Similar to non-pregnant uteri, KCl-induced contraction

was inversely decreased as its concentration was increased further to 120 mM (which was at 48.5 ±

4.6% of the 60 mM KCl-induced contraction) (Figure 3B). This biphasic contraction response to KCl

was detected in TMEM16A[SMKO] mice, and no difference was detected between the CTR and

TMEM16A[SMKO] mice (Figure 3B).

Smooth muscle cell-specific TMEM16A deletion causes no change in OT- and PGF2α-induced

contraction.

Oxytocin (OT) and PGF2α are two of the most important hormones regulating uterine

contractility in both non-pregnant and pregnant stages, we therefore studied whether TMEM16A

deletion in smooth muscle cells exert any effects on OT- and PGF2α-induced uterine contraction. In

CTR mice at estrus, OT and PGF2α induced dose-dependent contractions (Figures 4A and 5A). In

uteri (at those same stages) from TMEM16A[SMKO] mice, both agonists also caused dose-dependent

contractions, and moreover, the dose-response curves were not different compared to those from the

CTR mice (Figures 4A and 5A).

Compared to the circular uterine rings from mice at estrus, 60 mM KCl generated a similar force

in the longitudinal uterine strips from day 18 pregnant mice. Using 60 mM KCl as a reference, we

found that uteri strips from day 18 pregnant mice generated stronger force in response to OT in both CTR mice and TMEM16A^{SMKO} compared to those from mice at estrus (Figure 4B vs Figure 4A), but dose-force response curves to OT between CTR mice and TMEM16A^{SMKO} mice were not significantly different (Figure 4B). In day 18 pregnant mice, PGF2α generated the same magnitude force, but dose-force response curves were right-shifted compared to mice at estrus (Figure 5B vs Figure 5A). However, there was no significant difference in dose-force response curve between CTR and TMEM16A^{SMKO} mice (Figure 5A and 5B).

Smooth muscle cell-specific TMEM16A deletion produces no effect on KCl-, OT- and PGF2α-induced rise in intracellular Ca^{2+} in USM cells from day 18 pregnant mice.

Ca^{2+} is the primary signal for USM contraction and a ligand for TMEM16A, we hence tested whether the KCl- or agonist-induced increase in intracellular Ca^{2+} concentration [Ca^{2+}]$_i$ was impaired in TMEM16A^{SMKO} mice. Since no difference in the contraction of non-pregnant and pregnant uteri was detected in TMEM16A^{SMKO} mice, and isolation of single USM cells was much easier from day 18 pregnant mice, we focused on examining the Ca^{2+} signal in the USM cells from longitudinal myometrium at this stage of mice. KCl at 60 mM markedly increased [Ca^{2+}]$_i$ often in an oscillating pattern. To simplify the analysis, we compared the maximal peak Ca^{2+} signal in the train of Ca^{2+} oscillations. As shown in Figure 6A, there was no significant difference in the peak Ca^{2+} rise upon stimulation with KCl when TMEM16A was deleted. PGF2α at 3 µM produced a similar oscillating Ca^{2+} response as KCl (Figure 6B). TMEM16A deletion neither altered this pattern nor changed the peak Ca^{2+} rise in response to PGF2α. Interestingly, OT at 100 nM elicited a sustained rise in [Ca^{2+}]$_i$, and this rise was not changed when TMEM16A was deleted (Figure 6C).

TMEM16A^{SMKO} mice have normal gestation duration and litter size.

As smooth muscle cell TMEM16A deletion results in hypotension (25), we assessed whether there was a change in reproduction in TMEM16A^{SMKO} mice. TMEM16A KO mice had a gestation of approximately 19 days, which was not different from the CTR mice (Table 1). These KO mice had a litter size of 7 pups, which also was not different from the CTR mice (Table 1).

Discussion

Identifying ion channel genes that are required for uterine contraction is essential to understand uterine function and reproduction. In this study, using an integrative approach of molecular biology, genetics, and physiology, we firmly established that *Tmem16a* is not the gene encoding CaCCs in mouse USM cells. We have several lines of evidence to support this conclusion. First, when TMEM16A is specifically deleted in smooth muscle cells, myometrium generates the same spontaneous and agonist-induced contraction compared to the myometrium from isogenic control mice. Second, smooth muscle cell-specific TMEM16A deletion does not alter isolated single USM cell $[Ca^{2+}]_i$ responses upon stimulation via depolarization or contractile agonists oxytocin and PGF2α. Third, smooth muscle cell-specific TMEM16A deletion does not impair mouse reproduction in terms of their gestation duration and litter size. Fourth, immunostaining with a specific antibody for TMEM16A could not detect TMEM16A expression in USM cells from both isogenic control mice and *Tmem16a* knockout mice. This failure in detecting TMEM16A in USM cells is not due to the TMEM16A antibody used because the same antibody showed robust staining signals in endometrial stromal cells (see below) in the same tissue.

A major strengthen of this study is its use of smooth muscle cell-specific TMEM16A knockout cells and mice. Previous studies have depended on using CaCC inhibitors (e.g. niflumic acid) or TMEM16A inhibitor benzbromarone to infer the involvement of this gene in uterine contraction (9, 10, 16, 17, 26). CaCC inhibitors such as niflumic acid are well known to have off-target nonspecific effects. For example, in addition to inhibiting CaCCs, niflumic acid blocks or activates many other ion channels including big-conductance Ca^{2+}-activated K^+ channels in smooth muscle cells (27-30). Benzbromarone is a newly identified TMEM16A inhibitor (31). But this compound can also activate the Kv7 (KCNQ) K^+ channel family, inhibit CFTR chloride channels, and alter mitochondrial function and structure (32-34). Considering the non-specific effects of these pharmacological inhibitors, we took a genetic approach to specifically delete TMEM16A. TMEM16A is widely expressed in many cell types including nerve system, epithelial cells, secretory cells and smooth muscle, and its global deletion results in mouse death shortly after their birth (21-23, 35, 36). Therefore, we used a line of mice whose

TMEM16A in smooth muscle cells are specifically deleted with the LoxP-Cre system. A potential drawback for this system is the insufficient activity of Cre to delete the gene of interest in targeted cells. We confirmed that the Cre line used in this study effectively deletes TMEM16A in smooth muscle cells, and moreover, the same TMEM16A deletion abolishes Ca^{2+}-activated Cl^- currents in smooth muscle cells from airway and internal anal sphincter (18, 19). Therefore, our genetic approach provides compelling evidence that TMEM16A is neither expressed and nor functional in mouse USM cells in both pregnant and non-pregnant stages.

The uterus is a myogenic and spontaneously active organ. A major unresolved question about this organ relates to the cell types and cellular mechanisms of the pacemaker underlying this autonomic contractile behavior. One potential cell type and mechanism is that CaCCs in USM cells function as a pacemaking channel (7, 37, 38). As smooth muscle cells have a reversal potential for Cl^- around -25 mV which is less negative than the resting membrane potential (e.g., -60 mV), activation of CaCCs is expected to generate a current that would depolarize the membrane beyond the threshold of its action potential. Our present study indicates if this mechanism works in the uterus, TMEM16A is not the CaCC channel which generates this pacemaking current in USM cells as myometrial tissues from TMEM16A[SMKO] mice exert the same spontaneous contraction compared with the isogenic control mice. Another possibility for the uterine pacemaking could be due to the TMEM16A CaCCs in the interstitial cells of Cajal (ICCs) or PDGFRα^{+} cells as in the gut (39, 40). However, the presence of ICCs or ICC-like cells in the uterus has been highly controversial and remain to be settled (41-44). Importantly, ICC-like cells in the uterus do not generate spontaneous currents(42), a characteristic of the pacemaking current, and uterine cells don't express TMEM16A(45). Hence TMEM16A is most likely not the channel which produces pacemaking currents in these cells.

Uterine contraction is under tight control by endocrine and paracrine hormones. Among these hormones, oxytocin and PGF2α are two of the most important ones regulating uterine contraction during both pregnant and non-pregnant stages and during labor. Oxytocin and PGF2α activate oxytocin receptor (OTR) and PGF2α receptor (PTGFR) in USM cells, respectively. Activation of these two

receptors turns on a canonical Gq/11-mediated signaling pathway, leading to a rise in intracellular Ca^{2+}. This rise in Ca^{2+} can activate CaCCs which in turn functionally couples with voltage gated Ca^{2+} channels or ORAI Ca^{2+} influx channels (46-48). Should TMEM16A CaCCs be present in USM cells, we would expect to observe that the oxytocin- and PGF2α-induced rise in intracellular Ca^{2+} and/or contraction would be suppressed in our KO experiments. Yet, our experiments in TMEM16A^{-/-} cells and uterine tissues do not show this.

A significant finding in this study is that TMEM16A is expressed in the endometrium. Although the cell type(s) expressing TMEM16A in the endometrium is yet to be determined, the TMEM16A immunostaining pattern suggests that these cells are not luminal endometrial epithelial cells, instead they are likely to be stromal cells. This raises a possibility that TMEM16A in these cells may play an important reproductive function. Indeed, a very recent study found that TMEM16A is upregulated during embryo implantation and decidualization, and pharmacological inhibition of TMEM16A impairs these two processes in mice (49). It would be highly significant to identify the stromal cell type that expresses TMEM16A, determine the role of TMEM16A in the stromal cells in embryo implantation and decidualization, and delineate the molecular mechanisms by which TMEM16A may mediate these reproductive processes.

In conclusion, mouse USM cells from both non-pregnant and pregnant stages do not express TMEM16A CaCC channels, and these cells do not use this channel to generate spontaneous and agonist-induced contraction relating to reproduction. Since TMEM16A is robustly expressed in mouse endometrial stromal cells, it is likely this gene may play an important role in reproduction processes such as embryo implantation and decidualization. Whether our findings in mice can translate to human myometrium warrants further investigation.

Conflict of Interest Statement

The authors declare no potential conflicts of interest

References

1. Kunz G & Leyendecker G (2002) Uterine peristaltic activity during the menstrual cycle: characterization, regulation, function and dysfunction. *Reprod Biomed Online* 4 Suppl 3:5-9.
2. Bulletti C*, et al.* (2004) The patterns of uterine contractility in normal menstruating women: from physiology to pathology. *Ann N Y Acad Sci* 1034:64-83.
3. Aguilar HN & Mitchell BF (2010) Physiological pathways and molecular mechanisms regulating uterine contractility. *Hum Reprod Update* 16(6):725-744.
4. Garfield RE & Maner WL (2007) Physiology and electrical activity of uterine contractions. *Seminars in cell & developmental biology* 18(3):289-295.
5. Smith R, Imtiaz M, Banney D, Paul JW, & Young RC (2015) Why the heart is like an orchestra and the uterus is like a soccer crowd. *Am J Obstet Gynecol* 213(2):181-185.
6. Sanborn BM (2000) Relationship of ion channel activity to control of myometrial calcium. *J Soc Gynecol Investig* 7(1):4-11.
7. Wray S*, et al.* (2015) Progress in understanding electro-mechanical signalling in the myometrium. *Acta Physiol (Oxf)* 213(2):417-431.
8. Adaikan PG & Adebiyi A (2005) Effect of functional modulation of Ca2+-activated Cl-currents on gravid rat myometrial activity. *Indian journal of pharmacology* 37(1):21.
9. Dodds KN, Staikopoulos V, & Beckett EA (2015) Uterine Contractility in the Nonpregnant Mouse: Changes During the Estrous Cycle and Effects of Chloride Channel Blockade. *Biol Reprod* 92(6):141.
10. Mijušković A*, et al.* (2015) Chloride channels mediate sodium sulphide‐induced relaxation in rat uteri. *British journal of pharmacology* 172(14):3671-3686.
11. Young RC & Bemis A (2009) Calcium-activated chloride currents prolongs the duration of contractions in pregnant rat myometrial tissue. *Reprod Sci* 16(8):734-739.
12. Jones K, Shmygol A, Kupittayanant S, & Wray S (2004) Electrophysiological characterization and functional importance of calcium-activated chloride channel in rat uterine myocytes. *Pflügers Archiv* 448(1):36-43.
13. Song J*, et al.* (2009) Cloning and characterization of a calcium-activated chloride channel in rat uterus. *Biology of reproduction* 80(4):788-794.
14. Mundhenk L*, et al.* (2012) mCLCA3 Does Not Contribute to Calcium-Activated Chloride Conductance in Murine Airways. *American Journal of Respiratory Cell and Molecular Biology* 47(1):87-93.
15. Mundhenk L*, et al.* (2006) Both cleavage products of the mCLCA3 protein are secreted soluble proteins. *The Journal of biological chemistry* 281(40):30072-30080.
16. Bernstein K*, et al.* (2014) Calcium-activated chloride channels anoctamin 1 and 2 promote murine uterine smooth muscle contractility. *Am J Obstet Gynecol* 211(6):688. e681-688. e610.
17. Hyuga S*, et al.* (2018) Functional comparison of anoctamin 1 antagonists on human uterine smooth muscle contractility and excitability. *Journal of Smooth Muscle Research* 54:28-42.
18. Zhang C-H*, et al.* (2016) The molecular basis of the genesis of basal tone in internal anal sphincter. *Nature communications* 7:11358.
19. Zhang C-H*, et al.* (2013) The transmembrane protein 16A Ca2+-activated Cl− channel in airway smooth muscle contributes to airway hyperresponsiveness. *American journal of respiratory and critical care medicine* 187(4):374-381.
20. Gomez-Pinilla PJ*, et al.* (2009) Ano1 is a selective marker of interstitial cells of Cajal in the human and mouse gastrointestinal tract. *Am J Physiol Gastrointest Liver Physiol* 296(6):G1370-1381.

21. Caputo A*, et al.* (2008) TMEM16A, a membrane protein associated with calcium-dependent chloride channel activity. *Science* 322(5901):590-594.

22. Schroeder BC, Cheng T, Jan YN, & Jan LY (2008) Expression cloning of TMEM16A as a calcium-activated chloride channel subunit. *Cell* 134(6):1019-1029.

23. Yang YD*, et al.* (2008) TMEM16A confers receptor-activated calcium-dependent chloride conductance. *Nature* 455(7217):1210-1215.

24. Shankman LS*, et al.* (2015) KLF4-dependent phenotypic modulation of smooth muscle cells has a key role in atherosclerotic plaque pathogenesis. *Nat Med* 21(6):628-637.

25. Heinze C*, et al.* (2014) Disruption of vascular Ca2+-activated chloride currents lowers blood pressure. *J Clin Invest* 124(2):675-686.

26. Young RC & Bemis A (2009) Calcium-activated chloride currents prolongs the duration of contractions in pregnant rat myometrial tissue. *Reprod Sci* 16(8):734-739.

27. Pacaud P, Loirand G, Lavie JL, Mironneau C, & Mironneau J (1989) Calcium-activated chloride current in rat vascular smooth muscle cells in short-term primary culture. *Pflugers Arch* 413(6):629-636.

28. Janssen LJ & Sims SM (1992) Acetylcholine activates non-selective cation and chloride conductances in canine and guinea-pig tracheal myocytes. *J Physiol* 453:197-218.

29. Greenwood I & Large W (1995) Comparison of the effects of fenamates on Ca‐activated chloride and potassium currents in rabbit portal vein smooth muscle cells. *British journal of pharmacology* 116(7):2939-2948.

30. Li L*, et al.* (2008) Niflumic acid hyperpolarizes smooth muscle cells via calcium‐activated potassium channel in spiral modiolar artery of guinea pigs 1. *Acta pharmacologica Sinica* 29(7):789-799.

31. Huang F*, et al.* (2012) Calcium-activated chloride channel TMEM16A modulates mucin secretion and airway smooth muscle contraction. *Proc Natl Acad Sci U S A* 109(40):16354-16359.

32. Kaufmann P*, et al.* (2005) Mechanisms of benzarone and benzbromarone-induced hepatic toxicity. *Hepatology* 41(4):925-935.

33. Lan X*, et al.* (2016) Grafting voltage and pharmacological sensitivity in potassium channels. *Cell Res* 26(8):935-945.

34. Diena T*, et al.* (2007) Block of CFTR-dependent chloride currents by inhibitors of multidrug resistance-associated proteins. *Eur J Pharmacol* 560(2-3):127-131.

35. Rock JR, Futtner CR, & Harfe BD (2008) The transmembrane protein TMEM16A is required for normal development of the murine trachea. *Developmental biology* 321(1):141-149.

36. Ji Q*, et al.* (2018) Recent advances in TMEM16A: Structure, function, and disease. *J Cell Physiol*.

37. Young RC (2018) The uterine pacemaker of labor. *Best Practice & Research Clinical Obstetrics & Gynaecology*.

38. Young RC (2007) Myocytes, myometrium, and uterine contractions. *Annals of the new york academy of sciences* 1101(1):72-84.

39. McHale N, Hollywood M, Sergeant G, & Thornbury K (2006) Origin of spontaneous rhythmicity in smooth muscle. *J Physiol* 570(Pt 1):23-28.

40. Malysz J*, et al.* (2017) Conditional genetic deletion of Ano1 in interstitial cells of Cajal impairs Ca(2+) transients and slow waves in adult mouse small intestine. *Am J Physiol Gastrointest Liver Physiol* 312(3):G228-G245.

41. Radu BM*, et al.* (2017) Calcium Signaling in Interstitial Cells: Focus on Telocytes. *Int J Mol Sci* 18(2).

42. Duquette RA*, et al.* (2005) Vimentin-positive, c-kit-negative interstitial cells in human and rat uterus: a role in pacemaking? *Biol Reprod* 72(2):276-283.

43. Hutchings G, Williams O, Cretoiu D, & Ciontea SM (2009) Myometrial interstitial cells and the coordination of myometrial contractility. *J Cell Mol Med* 13(10):4268-4282.

44. Allix S*, et al.* (2008) Uterine contractions depend on KIT-positive interstitial cells in the mouse: genetic and pharmacological evidence. *Biol Reprod* 79(3):510-517.

45.   Peri LE*, et al.* (2015) A novel class of interstitial cells in the mouse and monkey female reproductive tracts. *Biol Reprod* 92(4):102.

46.   Sanborn BM (2007) Hormonal signaling and signal pathway crosstalk in the control of myometrial calcium dynamics. *Semin Cell Dev Biol* 18(3):305-314.

47.   Noble K, Matthew A, Burdyga T, & Wray S (2009) A review of recent insights into the role of the sarcoplasmic reticulum and Ca entry in uterine smooth muscle. *Eur J Obstet Gynecol Reprod Biol* 144 Suppl 1:S11-19.

48.   Concepcion AR*, et al.* (2016) Store-operated Ca2+ entry regulates Ca2+-activated chloride channels and eccrine sweat gland function. *J Clin Invest* 126(11):4303-4318.

49.   Qi Q, Yang Y, Wu K, & Xie Q (2018) Inhibition of TMEM16A impedes embryo implantation and decidualization in mice. *Reproduction* 156(6):569-577.
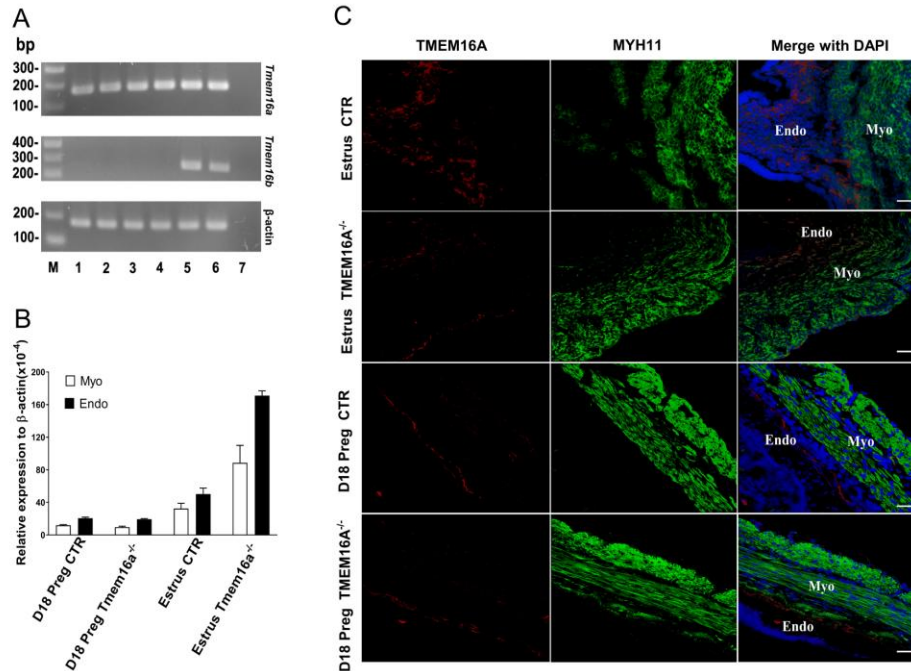
Figure 1. TMEM16A is expressed in endometrial stromal cells but not in myometrial cells. A. RT-PCR of Tmem16a and Tmem16B in endometrium and myometrium from estrus and day 18 pregnant CTR mice. M: Molecular marker, Lane 1: myometrium from day 18 pregnant mice, lane 2: endometrium from day 18 pregnant mice, lane 3: myometrium from estrus, lane 4: endometrium from estrus, lane 5: eye, lane 6: brain, lane 7: no primer negative control. Eye and brain were used as positive controls. **B.** Quantitative PCR analysis of TMEM16A mRNA in endometrium and myometrium from estrus and day 18 pregnant CTR and TMEM16A^{SMKO} mice. Bars represent mean ± SE, n=5 repeats. **C.** Co-immunostaining of TMEM16A and MYH11, a smooth muscle cell marker, in uteri from estrus and day 18 pregnant CTR and TMEM16A^{SMKO} mice. White bars equal 30 μm.
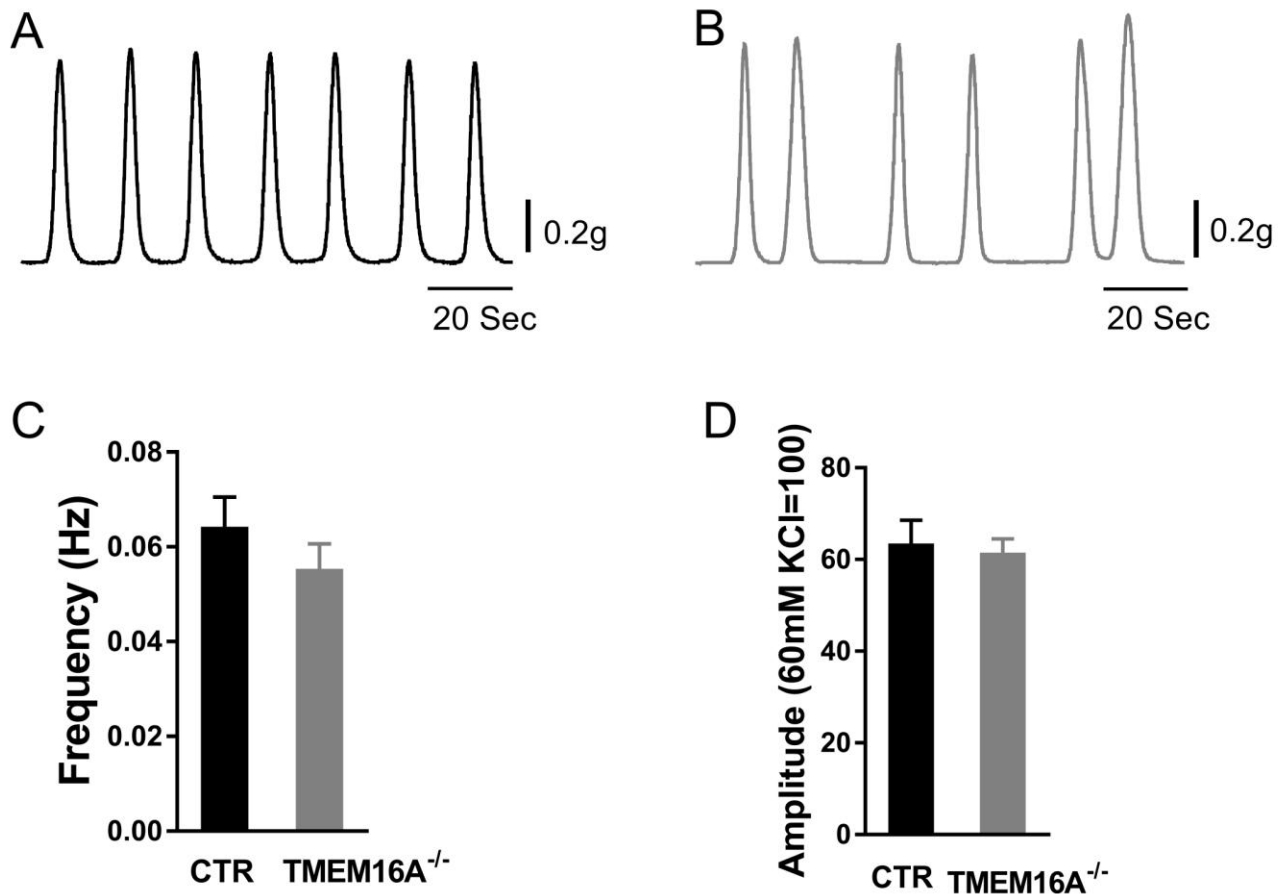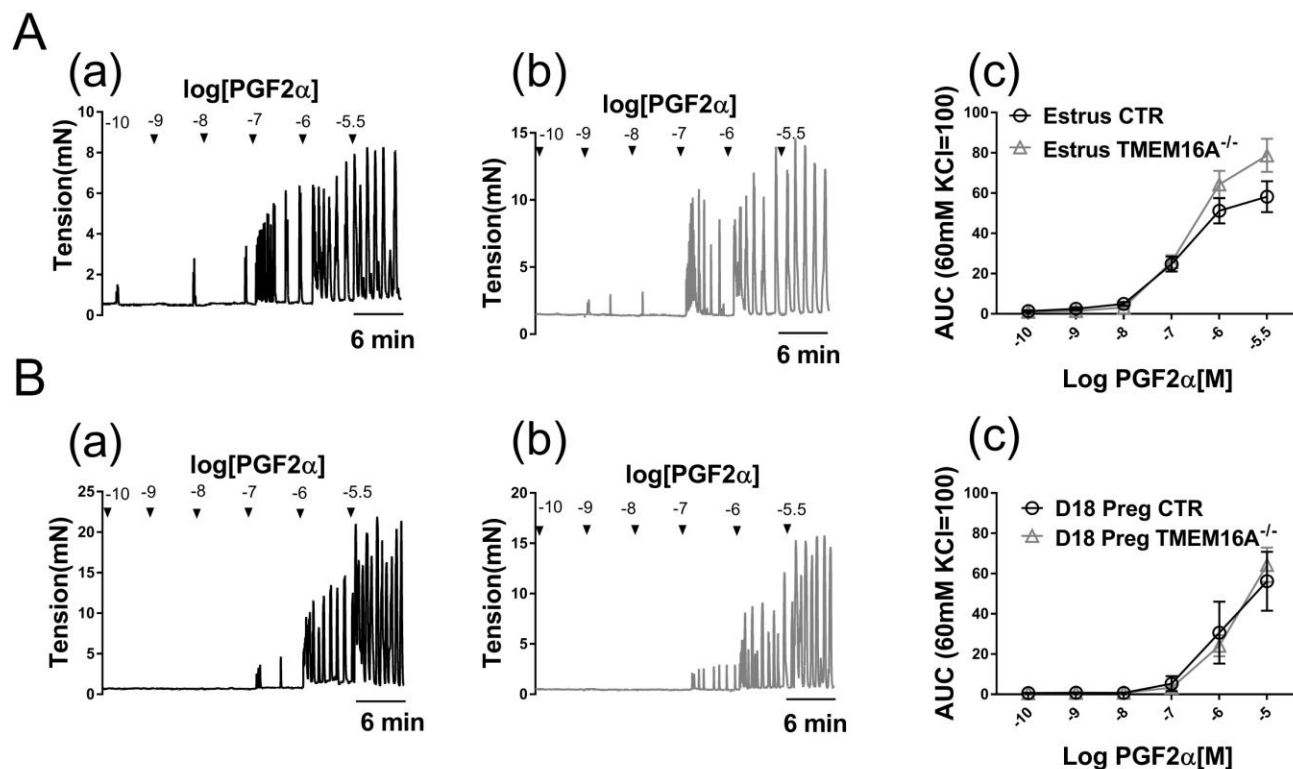
Figure 2. TMEM16A does not contribute to spontaneous uterine contraction in non-pregnant mice at estrus. A. B. Representative recordings of spontaneous contraction in circular myometrial rings from CTR mice (A) and TMEM16A^{SMKO} mice (B). **C, D.** Comparisons of the frequency (C) and amplitude (D) of spontaneous contraction between CTR mice and TMEM16A^{SMKO} mice. Bars represent mean ± SEM, n=20 strips from 5 mice; $P>0.05$ unpaired t-test CTR vs TMEM16A^{SMKO}.
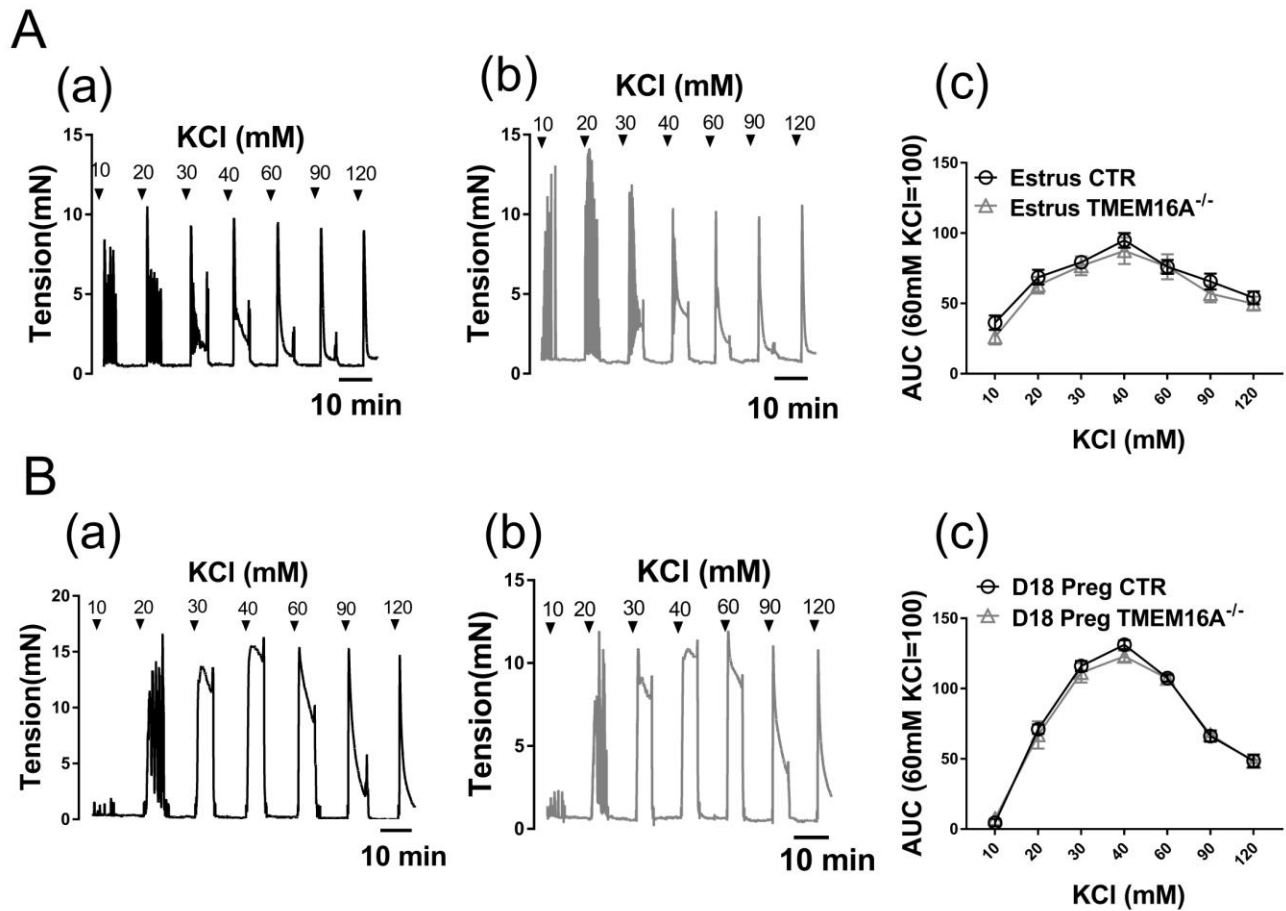
Figure 3. TMEM16A does not contribute to KCl-induced uterine contraction in non-pregnant and pregnant mice. A. A representative dose-force response upon stimulation with KCl in an estrus circular myometrial ring from a CTR mouse (a) and a TMEM16A[SMKO] mouse (b), and the summarized data (c) (Bars represent mean ± SEM, n=12 rings from 5 mice; P>0.05 ANOVA CTR vs TMEM16A[SMKO]). **B.** A representative dose-force response upon stimulation with KCl in a day 18-pregnant longitudinal myometrial strip from a CTR mouse (a) and a TMEM16A[SMKO] mouse (b), and the summarized data (c) (Data represent mean ± SEM, n= 8 strips from 4 mice; P>0.05 ANOVA CTR vs TMEM16A[SMKO]).
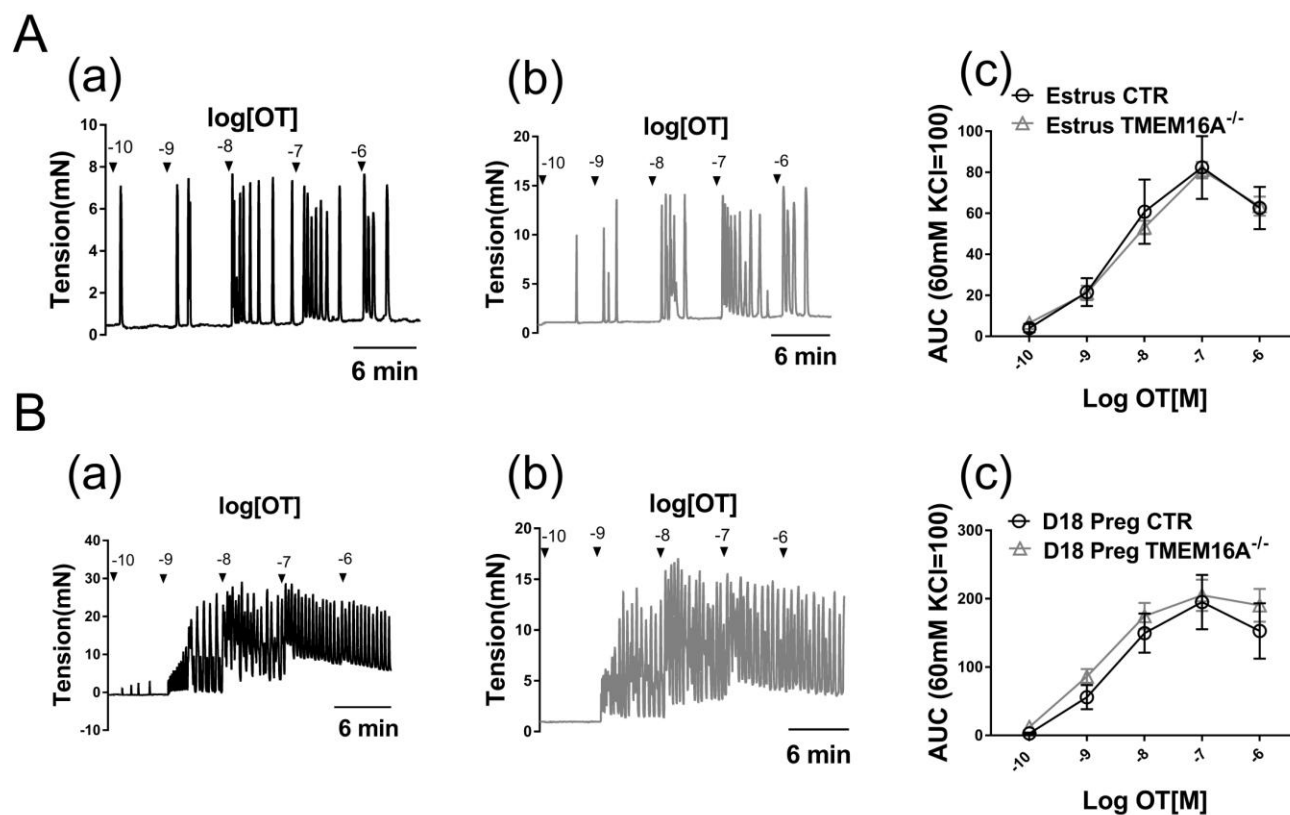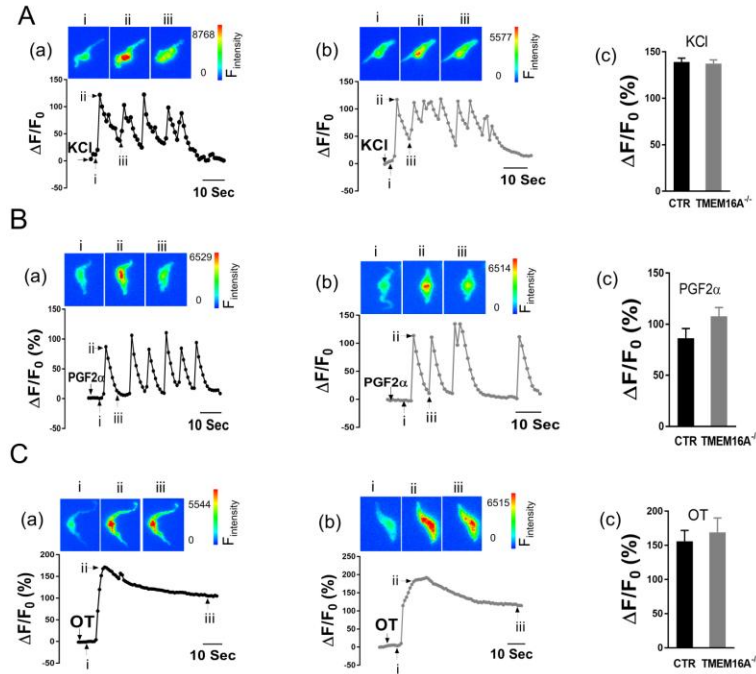
Figure 4. TMEM16A does not contribute to OT-induced uterine contraction in non-pregnant and pregnant mice. **A.** A representative dose-force response upon stimulation with oxytocin (OT) in an estrus circular myometrial ring from a CTR mouse (a) and a TMEM16A^{SMKO} mouse (b), and the summarized data (c) (Data represent mean ± SEM, n=8 rings from 4 mice; P>0.05 ANOVA CTR vs TMEM16A^{SMKO}). **B.** A representative dose-force response upon stimulation with OT in a day 18-pregnant longitudinal myometrial strip from a CTR mouse (a) and a TMEM16A^{SMKO} mouse (b), and the summarized data (c) (Data represent mean ± SEM, n=8 strips from 4 mice; P>0.05 ANOVA CTR vs TMEM16A^{SMKO}).

Figure 5. TMEM16A does not contribute to PGF2α-induced uterine contraction in non-pregnant and pregnant mice.

A. A representative dose-force response upon stimulation with PGF2α in an estrus circular myometrial ring from a WT mouse (a) and a TMEM16A[SMKO] mouse (b), and the summarized data (c) (Data represent mean ± SEM, n=8 rings from 4 mice; P>0.05 ANOVA CTR vs TMEM16A[SMKO]). **B.** A representative dose-force response upon stimulation with PGF2α in a day 18-pregnant longitudinal strip from a CTR mouse (a) and a TMEM16A[SMKO] mouse (b), and the summarized data (c) (Data represent mean ± SEM, n=8 strips from 4 mice; P>0.05 ANOVA CTR vs TMEM16A[SMKO]).

Figure 6. TMEM16A does not contribute to KCl- and contractile agonist-induced rise in intracellular Ca^{2+} concentration in day 18-pregnant myometrial cells. A. A representative Ca^{2+} response upon stimulation with KCl in a day 18-pregnant smooth muscle cell freshly isolated from longitudinal myometrium from a CTR mouse (a) and a TMEM16A^{SMKO} mouse (b), and the summarized data (c) (Bars represent mean ± SEM, n=20 cells from 3 mice; P>0.05 unpaired t-test CTR vs TMEM16A^{SMKO}). Images shown were expressed as fluorescence intensity and were taken at the time marked in the $\Delta F/F_0$ traces below. The same convention is applied to the images in B and C. **B.** A representative Ca^{2+} response upon stimulation with PGF2α in a day 18-pregnant smooth muscle cell freshly isolated from longitudinal myometrium from a CTR mouse (a) and a TMEM16A^{SMKO} mouse (b), and the summarized data (c) (Bars represent mean ± SEM, n=20 cells from 3 mice; P>0.05 unpaired t-test CTR vs TMEM16A^{SMKO}). **C.** A representative Ca^{2+} response upon stimulation with oxytocin (OT) in a day 18-pregnant smooth muscle cell freshly isolated from longitudinal myometrium from a CTR mouse (a) and a TMEM16A^{SMKO} mouse (b), and the summarized data (c) (Bars represent mean ± SEM, n=20 cells from 3 mice; P>0.05 unpaired t-test CTR vs TMEM16A^{SMKO}).

Table 1. Smooth muscle specific TMEM16A deletion does not alter gestation duration and litter size.

	CTR	TMEM16A^{SMKO}	
Gestation (day)	19 ± 0.5	19.3 ± 0.5	p>0.05
# pups/litter	7.9 ± 0.7	6.9 ± 0.4	p>0.05
N (mouse)	20	24	